

Highly enantioselective S–H bond insertion cooperatively catalyzed by dirhodium complexes and chiral spiro phosphoric acids†

Cite this: *Chem. Sci.*, 2014, 5, 1442Bin Xu,^a Shou-Fei Zhu,^{*a} Zhi-Chao Zhang,^a Zhi-Xiang Yu,^{*b} Yi Ma^a and Qi-Lin Zhou^{*a}

The first highly enantioselective S–H bond insertion reaction was developed by cooperative catalysis of dirhodium(II) carboxylates and chiral spiro phosphoric acids (SPAs) under mild and neutral reaction conditions with fast reaction rates, high yields (77–97% yields), and excellent enantioselectivities (up to 98% ee). The catalytic S–H bond insertion reaction provides a highly efficient method for the synthesis of chiral sulfur-containing compounds and advances the synthesis of a chiral sulfur-containing drug (S)-Eflucimibe. A systematic ³¹P NMR study revealed that no ligand exchange between dirhodium(II) carboxylates and SPAs occurred in the reaction. The distinct behaviors of cooperative catalysts Rh₂(TPA)₄/(R)-1a and the prepared complex Rh₂(R-1a)₄ observed by *in situ* FT-IR spectroscopy excluded the feasibility of Rh₂(R-SPA)₄ being the real catalyst. DFT calculations showed that the activation barrier in the proton shift step became remarkably low as promoted by SPAs. Based on the experimental results and the calculations, the SPA was proposed as a chiral proton shuttle for the proton shift in reaction. Additionally, the single crystal structures of several SPAs were measured and used to rationalize the configurations of the S–H insertion products obtained in the reactions. The rigid and crowded environment around the SPAs ensures the high enantioselectivity in the S–H bond insertion reaction.

Received 9th October 2013
Accepted 27th November 2013

DOI: 10.1039/c3sc52807c

www.rsc.org/chemicalscience

Introduction

The construction of carbon–heteroatom bonds is an essential task of organic synthesis, and many efficient methods, including enantioselective catalysis, have been developed for the formation of such bonds.¹ Many chiral sulfur-containing compounds have significant biological activities and are widely used as pharmaceuticals (Fig. 1).² More than one-fifth of the 200 most-prescribed pharmaceutical products in 2011 were sulfur-containing compounds,^{2a} and 22 of them, including Emtricitabine,^{2b} Diltiazem,^{2c} Montelukast,^{2d} Amoxicillin,^{2e} contained a chiral center bearing the C–S bond. To date, most chiral sulfur-containing compounds have been synthesized from other chiral compounds. For instance, chiral α -thiomandelic acid and

derivatives, which are versatile building blocks for the synthesis of bioactive compounds, are generally prepared from chiral α -halo- or α -hydroxy-carboxylic acid derivatives by means of stereospecific substitution reactions with sulfur nucleophiles.³ Although transition-metal-catalyzed S–H bond insertion reactions have been extensively studied and efficiently form C–S bonds under neutral reaction conditions, the progress on the asymmetric version of this reaction was limited.⁴ All the early attempts on enantioselective S–H bond insertion reactions with copper (up to 13.8% ee),^{4a} ruthenium (up to 8% ee),^{4b} and rhodium (up to 23% ee)^{4c} as catalysts exhibited very low enantioselectivities. Recently, we reported an enantioselective S–H bond insertion reaction catalyzed by copper complexes bearing chiral spiro bisoxazoline ligands.^{4d} However, the reaction afforded α -mercaptoesters in only moderate enantioselectivities (17–85% ee). The low chiral induction exhibited by transition metal catalysts in S–H bond insertion reactions has been attributed mainly to the high stability of the sulfonium ylide intermediate,⁵ which may permit degeneration of metal-associated ylide to free ylide and thus lead to low enantioselectivity. Here we report a highly enantioselective S–H insertion reaction cooperatively catalyzed by achiral dirhodium complex and chiral spiro phosphoric acids (SPAs), producing chiral α -mercaptoesters in high yields and excellent enantioselectivities (up to 98% ee).⁶ Detailed mechanism studies evidence a novel cooperative catalysis model, in which the achiral dirhodium generates a sulfonium ylide, and the chiral SPA controls the

^aState Key Laboratory and Institute of Elemento-organic Chemistry, Collaborative Innovation Center of Chemical Science and Engineering (Tianjin), Nankai University, Tianjin 300071, China. E-mail: sfzhu@nankai.edu.cn; qlzhou@nankai.edu.cn; Fax: +86-22-2350-6177

^bBeijing National Laboratory for Molecular Sciences (BNLMS), Key Laboratory of Bioorganic Chemistry and Molecular Engineering of the Ministry of Education, College of Chemistry, Peking University, Beijing 100871, China. E-mail: yuzx@pku.edu.cn

† Electronic supplementary information (ESI) available: Experimental procedures; spectral data for all new compounds; computational details. CCDC 960974 [(S)-4ca], 960978 [Rh₂(R-1a)₄(MeOH)₂], 960975 [(R)-1a], 960976 [(S)-1b], and 960977 [(R)-1f]. For ESI and crystallographic data in CIF or other electronic format see DOI: 10.1039/c3sc52807c

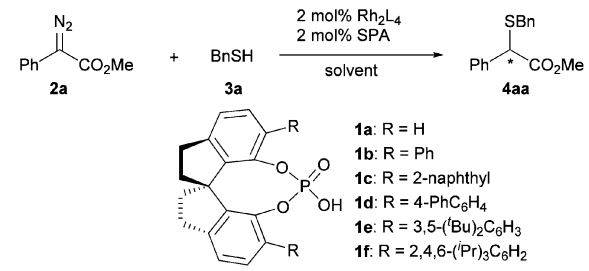
enantioselective 1,3-proton shift of enol *via* an eight-membered ring transition state.

Results and discussion

Initially, we studied the insertion of methyl α -diazo-phenylacetate (**2a**) into the S–H bond of benzyl mercaptan (**3a**) in CHCl_3 at 60 °C using $\text{Rh}_2(\text{OAc})_4$ and chiral SPA (*R*)-**1a** as the catalysts. The reaction completed in 5 min, and the desired S–H bond insertion product α -mercaptoester **4aa** was obtained in 78% yield with 16% ee (Table 1, entry 1). We next evaluated chiral SPAs with various substituents on the 6,6'-positions and found that (*R*)-**1f**, with bulky 6,6'-di-(2,4,6-tri-isopropylphenyl) moieties, gave the highest enantioselectivity (72% ee, entry 6). Variation of the dirhodium(II) carboxylates only slightly affected the yield and enantioselectivity of the reaction,⁷ with $\text{Rh}_2(\text{TPA})_4$ [tetrakis(triphenylacetato)dirhodium(II)] exhibiting the best performance (73% ee, entry 7). When the reaction temperature was lowered to 25 °C, the enantioselectivity was improved to 76% ee without compromising the yield or reaction rate (entry 8). The solvent strongly affected the enantioselectivity of reaction. When the reaction was performed in a non-polar, aprotic solvent such as benzene or cyclohexane (*c*-hexane) – both have better solubility for SPAs – the enantioselectivity was remarkably improved (86% ee and 93% ee, respectively; entries 9 and 10). In a sharp contrast, the highly-polar solvent THF slowed the reaction and eliminated the enantioselectivity (entry 11). When a slight excess (1.2 equiv.) of α -diazoacetate **2a** was used, the yield and enantioselectivity were further increased to 92% and 94% ee, respectively (entry 12).

We then investigated the substrate scope by carrying out reactions of various α -aryl- α -diazoesters with benzyl mercaptan (**3a**) under the optimized conditions. The electronic property of *para*- and *meta*-substituents on the aryl ring of diazoesters (**2b–g**) has a negligible impact on the yield and enantioselectivity: all the reactions completed in 5 min and produced the corresponding α -mercaptoesters in good yields (77–96%) and high enantioselectivities (90–96% ee) (Table 2, entries 1–7). In contrast, the enantioselectivity of the reaction of an *ortho*-methyl-substituted α -diazoester was low (58% ee, entry 8). In

Table 1 S–H insertion catalyzed by dirhodium(II) carboxylates and chiral spiro phosphoric acids: optimization of reaction conditions^a



Entry	Rh ₂ L ₄	SPAs	T (°C)	Solvent	Yield ^b (%)	ee ^c (%)
1	Rh ₂ (OAc) ₄	(<i>R</i>)- 1a	60	CHCl ₃	78	16
2	Rh ₂ (OAc) ₄	(<i>R</i>)- 1b	60	CHCl ₃	75	36
3	Rh ₂ (OAc) ₄	(<i>R</i>)- 1c	60	CHCl ₃	74	36
4	Rh ₂ (OAc) ₄	(<i>R</i>)- 1d	60	CHCl ₃	76	26
5	Rh ₂ (OAc) ₄	(<i>R</i>)- 1e	60	CHCl ₃	88	8
6	Rh ₂ (OAc) ₄	(<i>R</i>)- 1f	60	CHCl ₃	82	72
7	Rh ₂ (TPA) ₄	(<i>R</i>)- 1f	60	CHCl ₃	80	73
8	Rh ₂ (TPA) ₄	(<i>R</i>)- 1f	25	CHCl ₃	80	76
9	Rh ₂ (TPA) ₄	(<i>R</i>)- 1f	25	Benzene	75	86
10	Rh ₂ (TPA) ₄	(<i>R</i>)- 1f	25	Cyclohexane	86	93
11 ^d	Rh ₂ (TPA) ₄	(<i>R</i>)- 1f	25	THF	79	rac
12 ^e	Rh ₂ (TPA) ₄	(<i>R</i>)- 1f	25	Cyclohexane	92	94

^a Reaction conditions: Rh₂L₄/1/2a/3a = 0.004 : 0.004 : 0.2 : 0.2 (mmol) in 3 mL solvent. Reaction time: 5 min. ^b Isolated yield. ^c Determined by HPLC using a Chiralcel OD–H column. ^d The reaction completed in 6 h. ^e Using 1.2 equiv. of **2a**.

addition to diazo substrates with benzene rings, the substrates with fused rings such as 2-naphthyl, benzo[*d*][1,3]dioxol-5-yl, benzothiophenyl, and indolyl were tolerated in the reaction (entries 9–12). The S–H insertion product **4ca** was assigned to be (*S*)-configuration through the X-ray diffraction analysis of a single crystal (Fig. 2).⁸

Various mercaptans were also investigated in the S–H bond insertion reaction with methyl α -phenyl- α -diazoacetate (**2a**). The yields and enantioselectivities obtained with benzyl mercaptans containing an electron-donating group (**3b**) or an electron-withdrawing group (**3c**) at the *para*-position were similar to those obtained with **3a** (Table 3, entries 1–3). Mercaptans with an alkyl chain, such as *n*-dodecylmercaptan (**3d**),

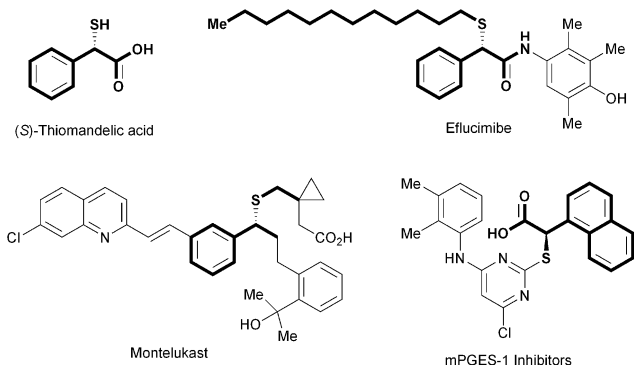


Fig. 1 Bioactive chiral sulfur-containing compounds.

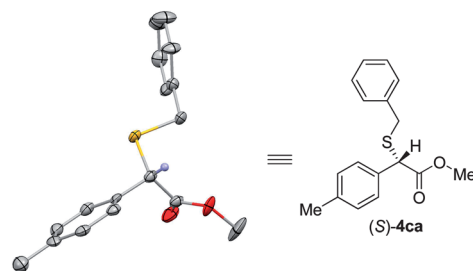
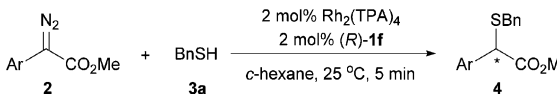
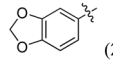
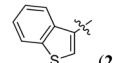
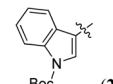


Fig. 2 The single crystal structure of (*S*)-**4ca**. H atoms, except the one at the chiral center, have been omitted for clarity.

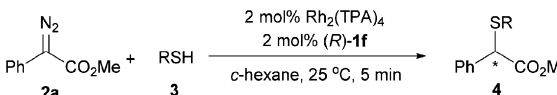
Table 2 S–H insertions of various α -aryl- α -diazoesters with benzyl mercaptan^a



Entry	Ar	Product	Yield (%)	ee (%)
1	Ph (2a)	4aa	92	94 (<i>S</i>) ^b
2	4-MeOC ₆ H ₄ (2b)	4ba	96	96
3	4-MeC ₆ H ₄ (2c)	4ca	96	95 (<i>S</i>)
4	4-ClC ₆ H ₄ (2d)	4da	90	93
5	3-MeOC ₆ H ₄ (2e)	4ea	90	91
6	3-MeC ₆ H ₄ (2f)	4fa	80	91
7	3-FC ₆ H ₄ (2g)	4ga	77	90
8	2-MeC ₆ H ₄ (2h)	4ha	90	58
9	2-Naphthyl (2i)	4ia	91	92
10	 (2j)	4ja	89	94
11	 (2k)	4ka	91	87
12	 (2l)	4la	96	90

^a The reaction conditions and analysis methods were the same as those described in Table 1, entry 12. ^b The absolute configuration was assigned by comparison with the reported optical rotation.⁹

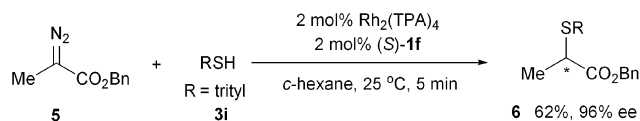
Table 3 S–H insertions of methyl α -phenyl- α -diazoesters with various mercaptans^a



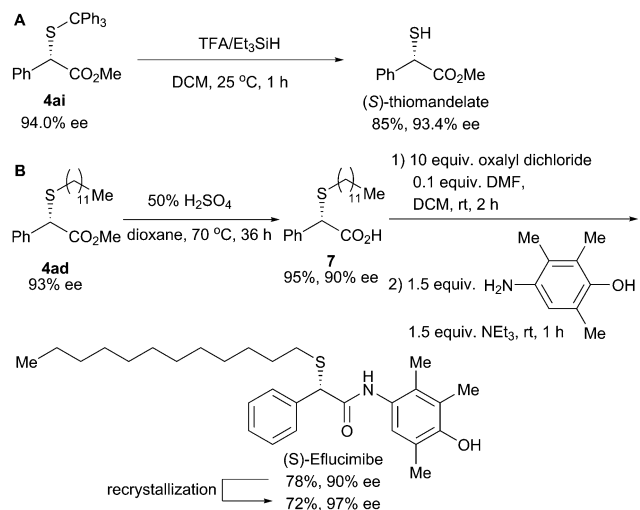
Entry	R	Product	Yield (%)	ee (%)
1	Bn (3a)	4aa	92	94 (<i>S</i>)
2	4-MeO-Bn (3b)	4ab	97	93
3	4-Cl-Bn (3c)	4ac	94	94
4	<i>n</i> -Dodecyl (3d)	4ad	86	93
5	<i>n</i> -Octyl (3e)	4ae	87	93
6	<i>n</i> -Pr (3f)	4af	86	93
7	<i>i</i> -Bu (3g)	4ag	89	87
8	<i>i</i> -Pr (3h)	4ah	89	78
9 ^b	Trityl (3i)	4ai	88	94
10	EtO ₂ CCH ₂ (3j)	4aj	83	98
11	2-Furylmethyl (3k)	4ak	85	96
12 ^b	4-MeOC ₆ H ₄ (3l)	4al	91	77

^a The reaction conditions and analysis methods were the same as those described in Table 1, entry 12. ^b Using (*S*)-1f.

n-octylmercaptan (3e), and *n*-propylmercaptan (3f), also afforded good yields and high enantioselectivities (entries 4–6), but the mercaptans with a bulkier *i*-butyl (3g) or *i*-propyl (3h) showed lower enantioselectivities (87% ee and 78% ee,



Scheme 1 Asymmetric S–H insertion of benzyl α -diazoacetate with tritylmercaptans.



Scheme 2 (A) Synthesis of optically active unprotected α -mercaptoester; (B) synthesis of (*S*)-Eflucimibe.

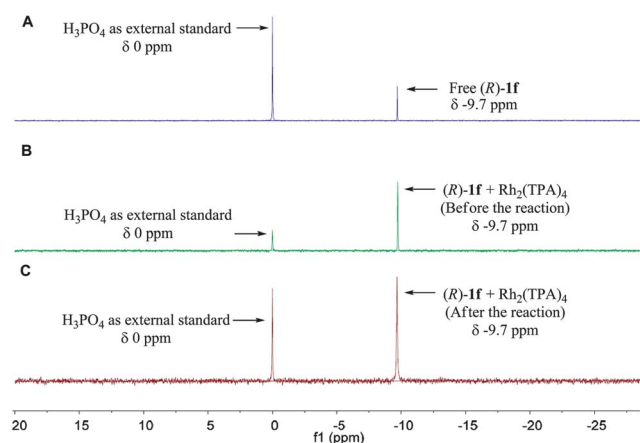
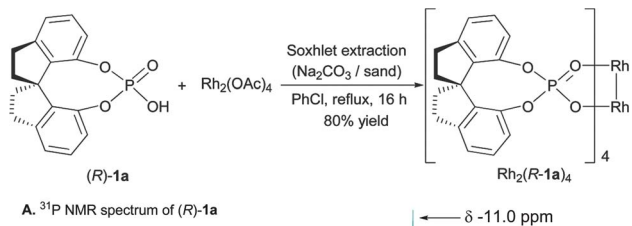


Fig. 3 ³¹P NMR measurements of SPA (*R*)-1f in CDCl₃ at 25 °C.

respectively; entries 7 and 8). Interestingly, the sterically hindered tritylmercaptan (3i) provided the desired S–H insertion product 4ai with high enantioselectivity (94% ee, entry 9). The ester (3j) and furan groups in the mercaptan (3k) were tolerated in the reaction (entries 10 and 11), and ethyl 2-mercaptoacetate (3j) showed the highest enantioselectivity (98% ee, entry 10). In addition to mercaptans, thiophenol 3l also underwent the S–H bond insertion reaction, although the enantioselectivity was only moderate (77% ee, entry 12).

The insertion reaction of benzyl α -diazoacetate (5), a typical α -alkyl- α -diazoester, with tritylmercaptan (3i) also gave excellent enantioselectivity (96% ee) (Scheme 1).



Scheme 3 Synthesis of $\text{Rh}_2(\text{R-1a})_4$ and the ^{31}P NMR spectra of (R) -1a and $\text{Rh}_2(\text{R-1a})_4$ in CDCl_3 at room temperature.

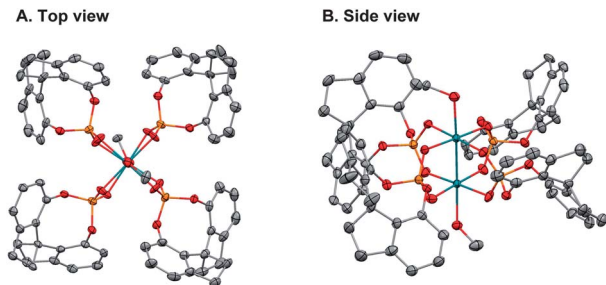


Fig. 4 X-ray structure of $\text{Rh}_2(\text{R-1a})_4(\text{MeOH})_2$. All H atoms and solvent molecules have been omitted for clarity.

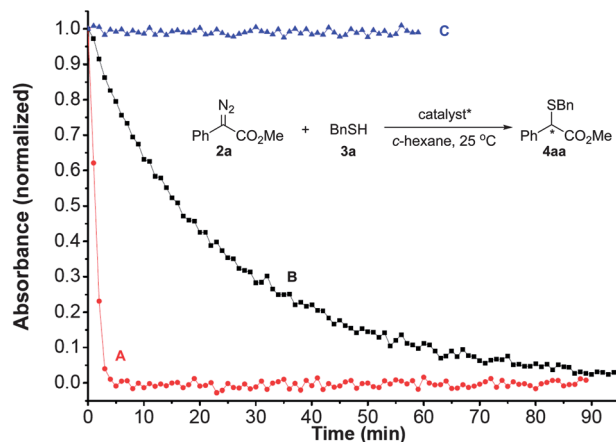


Fig. 5 The reactions of **2a** and **3a** monitored by *in situ* FT-IR spectroscopy. (A) 2 mol% $\text{Rh}_2(\text{TPA})_4$ and 2 mol% (R) -1a; (B) 2 mol% $\text{Rh}_2(\text{R-1a})_4$; (C) 2 mol% (R) -1a. The absorbances of the $\text{C}=\text{N}_2$ bond (2088 cm^{-1}) of α -diazoester **2a** were recorded.

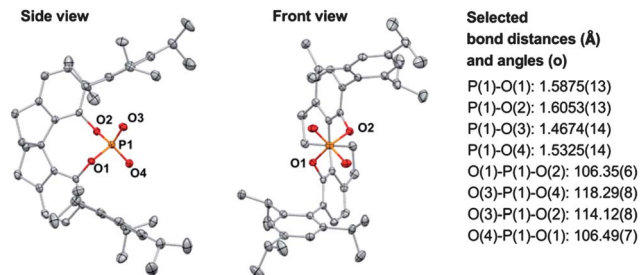


Fig. 6 X-ray structure of (R) -1f. All H atoms and solvent molecules have been omitted for clarity.

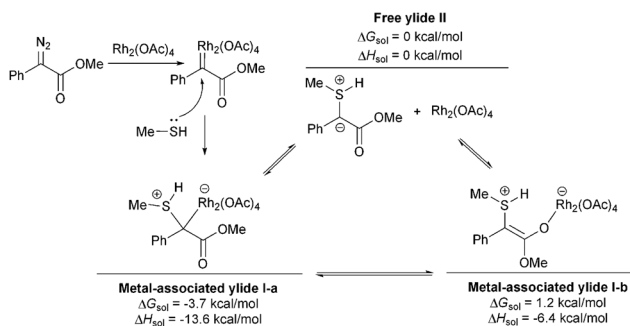


Fig. 7 DFT calculations on the relative free energies of three possible ylide intermediates.

The trityl group of insertion product **4ai** could be removed with Et_3SiH under mild conditions^{3b} to afford the corresponding α -mercaptoester with a free thiol group in 85% yield, and the optical purity was retained (Scheme 2A). The synthesis of (*S*)-Eflucimibe,¹⁰ a medicine for the treatment of atherosclerosis and lipoprotein disorders, was accomplished from the S-H insertion product **4ad** through hydrolysis and amidation steps (Scheme 2B). Although a slight drop of ee value (from 93% ee to 90% ee) was observed during the acidic hydrolysis, the optical purity of the final product (*S*)-Eflucimibe could be improved to 97% ee through a recrystallization.

We performed additional experiments to understand the cooperative catalysis in the S-H bond insertion reactions. Because chiral dirhodium(II) phosphate complexes were applied as catalysts for asymmetric carbene transformations¹¹ the possibility of chiral spiro dirhodium(II) phosphate complexes, which may be generated *in situ* during the reaction, catalyzing S-H insertion reaction was carefully considered. Firstly, control experiments were carried out to check if the ligand exchange between dirhodium(II) carboxylates and chiral phosphoric acids took place during the S-H insertion reaction. The ^{31}P NMR spectra of the catalysts before or after the S-H insertion reaction are identical to that of SPA (R) -1f (chemical shifts are -9.7 ppm in three cases, Fig. 3), which clearly indicated that no chiral dirhodium(II) phosphate complexes were formed under the reaction conditions.

We then tried to prepare the dirhodium(II) phosphate complexes of SPAs.¹¹ No dirhodium(II) phosphate complexes were detected by ^{31}P NMR even after heating the mixture of

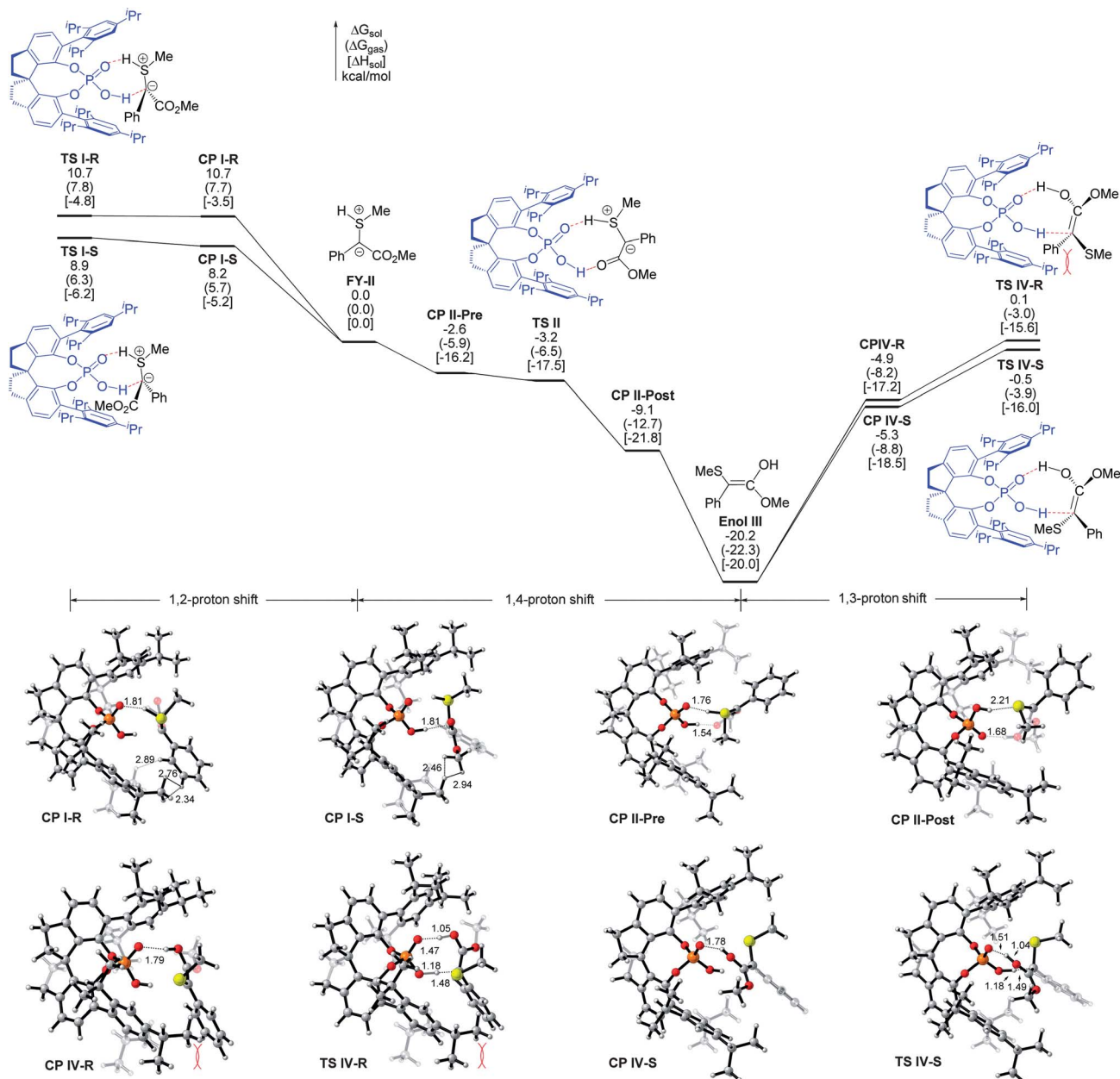


Fig. 8 The computed energy surfaces for the phosphoric acid-catalyzed proton shifts.

(*R*)-**1f** and $\text{Rh}_2(\text{OAc})_4$ in chlorobenzene at reflux for 20 h; only recovered (*R*)-**1f** was obtained. When a less bulky SPA (*R*)-**1a** reacted with $\text{Rh}_2(\text{OAc})_4$ at reflux for 16 h, the chiral dirhodium(II) phosphate complex $\text{Rh}_2(\text{R-1a})_4$ was formed in 80% yield as a blue-green solid (Scheme 3). The structure of $\text{Rh}_2(\text{R-1a})_4$ was confirmed by the X-ray diffraction analysis of its single crystal and the crowded environment around $\text{Rh}_2(\text{R-1a})_4$ may account for the failure in the preparation of analogous complexes with 6,6'-substituted SPAs (Fig. 4).⁸ The ^{31}P NMR of $\text{Rh}_2(\text{R-1a})_4$ has a remarkable shift to low field compared with that of free SPA (*R*)-**1a** (Scheme 3). The notable shift of the ^{31}P NMR between (*R*)-**1a** and $\text{Rh}_2(\text{R-1a})_4$ ($\Delta\delta = 16.3$ ppm) logically supported the judgment we made from the ^{31}P NMR control experiments in Fig. 3:

that no chiral dirhodium(II) phosphate complexes were formed in the S-H insertion reaction.

We investigated the catalytic activity of $\text{Rh}_2(\text{R-1a})_4$ in the S-H insertion reaction of α -diazoacetate **2a** with benzyl mercaptan **3a** monitoring by *in situ* FT-IR spectroscopy. As shown in Fig. 5, the reaction catalyzed by complex $\text{Rh}_2(\text{R-1a})_4$ finished within 90 min (line B) whereas the reaction cooperatively catalyzed by $\text{Rh}_2(\text{TPA})_4/(\text{R-1a})$ was completed within only 5 min (line A). The distinct difference between the reactions by using $\text{Rh}_2(\text{R-1a})_4$ and $\text{Rh}_2(\text{TPA})_4/(\text{R-1a})$ provided further evidence for ruling out $\text{Rh}_2(\text{R-1a})_4$ from the major catalytic species in the S-H insertion reaction catalyzed by $\text{Rh}_2(\text{TPA})_4/(\text{R-1a})$. No S-H insertion reaction was observed by using only (*R*)-**1a** (line C), which implied

that the S–H insertion reaction was catalyzed cooperatively by $\text{Rh}_2(\text{TPA})_4/(\text{R})\text{-1a}$ rather than by $(\text{R})\text{-1a}$ itself.

Although the applications of SPAs in organocatalysis were extensively studied in recent years,¹² the X-ray structures of SPAs remain unknown. We fortunately grew three single crystals of typical SPAs, $(\text{R})\text{-1a}$, $(\text{S})\text{-1b}$, and $(\text{R})\text{-1f}$.⁸ The X-ray diffraction analyses of these SPAs were taken and the structure of $(\text{R})\text{-1f}$ is shown in Fig. 6. The single crystal structures of SPAs facilitated the understanding of the chiral induction model of the S–H insertion reaction (*vide infra*).

We further performed density functional theory (DFT) calculations by the B3LYP/6-311+G(d,p)//B3LYP/6-31G(d) method in cyclohexane solution (using the PCM model) to gain more insight into the reaction mechanism of the cooperatively catalyzed S–H insertion reaction (calculations were performed using the Gaussian 09 program).⁷ Previous DFT calculations by Yu and co-workers indicated that free ylide is generated in O–H insertion reaction using Rh catalyst, due to the weak O–Rh bond between the substrate and the catalyst. Once the free ylide is generated, Yu proposed that water is involved to catalyze the [1,2]-proton shift.¹³ We hypothesized that, in the present system, free ylide also exists and chiral spiro phosphoric acid acts as a catalyst to catalyze the proton shift process, which also directs the enantioselectivity of the present S–H insertion reaction. Therefore, we tried first to know whether delivering the free ylide is favored or not (Fig. 7). Calculations found that the metal-associated ylide **I-a** (rhodium bonded at the carbon) is more stable than **I-b** (the enolate's oxygen coordinated to Rh) by 4.9 kcal mol⁻¹ in terms of Gibbs free energy in solution. Even though the binding enthalpy of the ylide and the catalyst is 13.6 kcal mol⁻¹, dissociation of **I-a** to the free ylide **II** and the catalyst is not difficult because this process is uphill by only 3.7 kcal mol⁻¹ in terms of Gibbs energy. This dissociation can be understandable because dissociation is favored entropically.

Once the free ylide is liberated, it could generate the final insertion products through two possible pathways (Fig. 8). One pathway involves an SPA-assisted [1,2]-proton shift as shown in the left-hand part of Fig. 8.^{14,15} In this pathway, the free ylide first forms two complexes with SPA $(\text{R})\text{-1f}$, that is **CP I-S** and **CP I-R**, which can undergo the concerted asymmetric [1,2]-proton shift processes with the assistance of $(\text{R})\text{-1f}$ to give the $(\text{S})\text{-product}$ and $(\text{R})\text{-product}$, respectively. The computed activation energies for these two processes are 8.9 kcal mol⁻¹ and 10.7 kcal mol⁻¹, respectively. The alternative plausible pathway involves tandem [1,4]-proton shift and [1,3]-proton shift processes as shown in the middle and right-hand parts in Fig. 8. The enol pathway from **FY II** to **CP II-Post** is favoured kinetically (with a negative activation free energy)¹⁶ and thermodynamically over the pathway *via* **TS I-R** and **TS I-S**. In the enol pathway, **CP II-Post** can undergo geometry changes to form complexes **CP IV-R** and **CP IV-S**, or it can decompose into enol (**Enol III**)¹⁷ and the catalyst, which then form complexes **CP IV-R** and **CP IV-S** for the final [1,3]-H shift to give the S–H insertion product. Calculations found that **CP IV-R** and **CP IV-S** undergo $(\text{R})\text{-1f}$ -catalyzed [1,3]-proton shifts *via* eight-membered transition states **TS IV-R** and **TS IV-S**, respectively. DFT calculations at the B3LYP/6-311+G(d,p)//B3LYP/6-31G(d) level indicated that **TS IV-S** is lower in energy than **TS IV-R** by

0.6 kcal mol⁻¹. This free energy difference can be increased to 1.7 kcal mol⁻¹ when the dispersion energy is considered by using the M06-2X/6-31G*//B3LYP/6-31G(d) calculation method.⁷ This suggests that final insertion product with *S* configuration was mainly generated from **TS IV-S**. In the disfavored transition state **TS IV-R**, the phenyl group of the enol experiences steric repulsion from the 2,4,6-triisopropylphenyl group of $(\text{R})\text{-1f}$, while these two groups are well parallel to each other in the favored transition state **TS IV-S**. Calculations using M06-2X above suggest that the dispersion interaction could be important for the experimentally observed enantioselectivity.¹⁸

Conclusions

In conclusion, the first highly enantioselective S–H insertion reaction was accomplished by using a cooperative catalysis of dirhodium(II) carboxylates and chiral SPAs. The dirhodium(II) carboxylate catalyzed the decomposition of diazo compounds to generate the sulfonium ylide, and the chiral SPAs promoted the proton shift-like proton shuttles and thus realized efficient chiral induction. Detailed investigations including ³¹P NMR on the SPAs in the reaction and X-ray diffraction on the single crystals of SPAs and the $\text{Rh}_2(\text{SPA})_4$, and the DFT calculations on the transition states evidenced this novel cooperative catalysis model. This catalytic asymmetric S–H insertion reaction provides a highly efficient method for the synthesis of chiral sulfur-containing compounds such as $(\text{S})\text{-thiomandelate}$ and $(\text{S})\text{-Eflucimibe}$. The cooperative catalysis exhibited unique advantages in the S–H bond insertion reaction and is expected to have wide applications in other asymmetric synthesis.

Acknowledgements

We thank the National Natural Science Foundation of China and the National Basic Research Program of China (2012CB821600), the “111” project (B06005) of the Ministry of Education of China, and the Program for New Century Excellent Talents in University (NCET-10-0516) for financial support.

Notes and references

- 1 A. K. Yudin, *Catalyzed Carbon–Heteroatom Bond Formation*, Wiley-VCH, Weinheim, 2011.
- 2 (a) The table of Top 200 Pharmaceutical Products by Total US Prescriptions in 2011, <http://www.pharmacytimes.com/publications/issue/2012/July2012/Top-200-Drugs-of-2011>; (b) M. Tisdale, S. D. Kemp, N. R. Parry and B. A. Larder, *Proc. Natl. Acad. Sci. U. S. A.*, 1993, **90**, 5653; (c) G. Sobal, E. J. Menzel and H. Sinzinger, *Biochem. Pharmacol.*, 2001, **61**, 373; (d) A. Halama, J. Jirman, O. Boušková, P. Gibala and K. Jarrah, *Org. Process Res. Dev.*, 2010, **14**, 425; (e) R. Suhas, S. Chandrashekar and D. C. Gowda, *Eur. J. Med. Chem.*, 2012, **48**, 179.
- 3 (a) B. Srijtveen and R. M. Kellogg, *J. Org. Chem.*, 1986, **51**, 3664; (b) R. L. Harding and T. D. H. Bugg, *Tetrahedron Lett.*, 2000, **41**, 2729; (c) S.-K. Lee, S.-Y. Lee and Y.-S. Park, *Synlett*, 2001, 1941; (d) J. Nam, S.-K. Lee, K.-Y. Kim and Y.-S. Park,

- Tetrahedron Lett.*, 2002, **43**, 8253; for a synthesis of chiral α -mercaptoesters through a dynamic kinetic resolution of the racemates, see: (e) X. Yang and V. B. Birman, *Angew. Chem., Int. Ed.*, 2011, **50**, 5553; for reviews on C–S bond constructions, see: (f) T. Kondo and T.-A. Mitsudo, *Chem. Rev.*, 2000, **100**, 3205; (g) I. P. Beletskaya and V. P. Ananikov, *Chem. Rev.*, 2011, **111**, 1596.
- 4 (a) H. Brunner, K. Wutz and M. P. Doyle, *Monatsh. Chem.*, 1990, **121**, 755; (b) E. Galardon, S. Roué, P. L. Maux and G. Simonneaux, *Tetrahedron Lett.*, 1998, **39**, 2333; (c) X.-M. Zhang, M. Ma and J.-B. Wang, *ARKIVOC*, 2003, **2003**, 84; (d) Y.-Z. Zhang, S.-F. Zhu, Y. Cai, H.-X. Mao and Q.-L. Zhou, *Chem. Commun.*, 2009, 5362; for reviews on asymmetric X–H bond insertion reactions, see: (e) M. P. Doyle, M. A. McKevey and T. Ye, *Modern Catalytic Methods for Organic Synthesis with Diazo Compounds*, Wiley, New York, 1998, ch. 8; (f) C. J. Moody, *Angew. Chem., Int. Ed.*, 2007, **46**, 9148; (g) S.-F. Zhu and Q.-L. Zhou, *Acc. Chem. Res.*, 2012, **45**, 1365; for selected examples on highly enantioselective O–H and N–H bond insertion reactions, see: (h) T. C. Maier and G. C. Fu, *J. Am. Chem. Soc.*, 2006, **128**, 4594; (i) C. Chen, S.-F. Zhu, B. Liu, L.-X. Wang and Q.-L. Zhou, *J. Am. Chem. Soc.*, 2007, **129**, 12616; (j) S.-F. Zhu, Y. Cai, H.-X. Mao, J.-H. Xie and Q.-L. Zhou, *Nat. Chem.*, 2010, **2**, 546; (k) S.-F. Zhu, X.-G. Song, Y. Li, Y. Cai and Q.-L. Zhou, *J. Am. Chem. Soc.*, 2010, **132**, 16374; (l) T. Osako, D. Panichakul and Y. Uozumi, *Org. Lett.*, 2012, **14**, 194; (m) B. Liu, S.-F. Zhu, W. Zhang, C. Chen and Q.-L. Zhou, *J. Am. Chem. Soc.*, 2007, **129**, 5834; (n) E. C. Lee and G. C. Fu, *J. Am. Chem. Soc.*, 2007, **129**, 12066; (o) Z.-R. Hou, J. Wang, P. He, J. Wang, B. Qin, X.-H. Liu, L.-L. Lin and X.-M. Feng, *Angew. Chem., Int. Ed.*, 2010, **49**, 4763; (p) S.-F. Zhu, B. Xu, G.-P. Wang and Q.-L. Zhou, *J. Am. Chem. Soc.*, 2012, **134**, 346; (q) X.-F. Xu, P. Y. Zavalij and M. P. Doyle, *Angew. Chem., Int. Ed.*, 2012, **51**, 9829.
- 5 (a) A.-H. Li, L.-X. Dai and V. K. Aggarwal, *Chem. Rev.*, 1997, **97**, 2341; (b) M. P. Doyle and D. C. Forbes, *Chem. Rev.*, 1998, **98**, 911.
- 6 For the asymmetric N–H bond insertion cooperatively catalyzed by rhodium and chiral spiro phosphoric acids, see: (a) B. Xu, S.-F. Zhu, X.-L. Xie, J.-J. Shen and Q.-L. Zhou, *Angew. Chem., Int. Ed.*, 2011, **50**, 11483; for other examples of asymmetric cooperative catalysis with transition metal/Brønsted acid, see: (b) V. Komanduri and M. J. Krische, *J. Am. Chem. Soc.*, 2006, **128**, 16448; (c) W.-H. Hu, X.-F. Xu, J. Zhou, W.-J. Liu, H.-X. Huang, J. Hu, L.-P. Yang and L.-Z. Gong, *J. Am. Chem. Soc.*, 2008, **130**, 7782; (d) Z.-Y. Han, H. Xiao, X.-H. Chen and L.-Z. Gong, *J. Am. Chem. Soc.*, 2009, **131**, 9182; (e) M. Rueping, R. M. Koenigs and I. Atodiresei, *Chem.–Eur. J.*, 2010, **16**, 9350; (f) J. Jiang, H.-D. Xu, J.-B. Xi, B.-Y. Ren, F.-P. Lv, X. Guo, L.-Q. Jiang, Z.-Y. Zhang and W.-H. Hu, *J. Am. Chem. Soc.*, 2011, **133**, 8428; (g) M. Terada and Y. Toda, *Angew. Chem., Int. Ed.*, 2012, **51**, 2093; (h) J. R. Zbieg, E. Yamaguchi, E. L. McInturff and M. J. Krische, *Science*, 2012, **336**, 324; (i) H. Qiu, D. Zhang, S.-Y. Liu, L. Qiu, J. Zhou, Y. Qian, C.-W. Zhai and W.-H. Hu, *Acta Chim. Sin.*, 2012, **70**, 2484.
- 7 See ESI† for details.
- 8 See Tables S2–10 in ESI† for details.
- 9 W. A. Bonner, *J. Org. Chem.*, 1967, **32**, 2496.
- 10 (a) D. Junquero, P. Oms, E. Carilla-Durand, J.-M. Autin, J.-P. Tarayre, A.-D. Degryse, J.-F. Patoiseau, F. C. Colpaert and A. Delhon, *Biochem. Pharmacol.*, 2001, **61**, 97; (b) J. Z.-L. José, F.-S. Ruth, J. L. F. Antonio, L.-T. Lucía, A.-O. Sergio, S. Daniel, J. Didier, D. André, C. Antonio, J. M.-C. Petra and M. Carlos, *J. Cardiovasc. Pharmacol.*, 2006, **48**, 128 and references cited therein.
- 11 (a) N. McCarthy, M. A. McKevery, T. Ye, M. McCann, E. Murphy and M. P. Doyle, *Tetrahedron Lett.*, 1992, **33**, 5983; (b) M. C. Pirrung and J. Zhang, *Tetrahedron Lett.*, 1992, **33**, 5987; (c) R. Hrdina, L. Guénée, D. Moraleda and J. Lacour, *Organometallics*, 2013, **32**, 473 and references cited therein.
- 12 (a) F. Xu, D. Huang, C. Han, W. Shen, X. Lin and Y. Wang, *J. Org. Chem.*, 2010, **75**, 8677; (b) I. Ćorić, S. Müller and B. List, *J. Am. Chem. Soc.*, 2010, **132**, 17370; (c) C.-H. Xing, Y.-X. Liao, J. Ng and Q.-S. Hu, *J. Org. Chem.*, 2011, **76**, 4125; (d) D. M. Rubush, M. A. Morges, B. J. Rose, D. H. Thamm and T. Rovis, *J. Am. Chem. Soc.*, 2012, **134**, 13554; (e) Z.-L. Chen, B.-L. Wang, Z.-B. Wang, G.-Y. Zhu and J.-W. Sun, *Angew. Chem., Int. Ed.*, 2013, **52**, 2027; (f) X.-J. Li, Y.-Y. Zhao, H.-J. Qu, Z.-J. Mao and X.-F. Lin, *Chem. Commun.*, 2013, **49**, 1401; (g) Q. Cai, X.-W. Liang, S.-G. Wang and S.-L. You, *Org. Biomol. Chem.*, 2013, **11**, 1602 and ref. 6a.
- 13 (a) Y. Liang, H.-L. Zhou and Z.-X. Yu, *J. Am. Chem. Soc.*, 2009, **131**, 17783. Yu and colleagues have found that the intramolecular [1,2]-proton shift and [1,3]-proton shift are difficult and these are usually catalyzed by a trace amount of water or other protonic solvents/reagents in the reaction systems: (b) Y. Xia, Y. Liang, Y. Chen, M. Wang, L. Jiao, F. Huang, S. Liu, Y. Li and Z.-X. Yu, *J. Am. Chem. Soc.*, 2007, **129**, 3470; (c) Y. Liang, S. Liu, Y. Xia, Y. Li and Z.-X. Yu, *Chem.–Eur. J.*, 2008, **14**, 4361; (d) Y. Liang, S. Liu and Z.-X. Yu, *Synlett*, 2009, 905.
- 14 (a) H. E. Helson and W. L. Jørgensen, *J. Org. Chem.*, 1994, **59**, 3841; (b) D. J. Miller and C. J. Moody, *Tetrahedron*, 1995, **51**, 10811; (c) M. P. Doyle and M. Yan, *Tetrahedron Lett.*, 2002, **43**, 5929; (d) See Chapter 8.1 in ref. 4e.
- 15 The direct proton shifts and the proton shifts promoted by other protonic sources, such as a trace amount of water or the thiol were also calculated. Our DFT calculations support that phosphoric acid (**R**)-**1f** acts as the real catalyst for the proton shift processes. See ESI† for details.
- 16 In terms of Gibbs free energy, **TS II** is lower by 0.6 kcal mol^{−1} than **CP II-Pre** in solution but is higher than **CP II-Pre** by 2.6 kcal mol^{−1} without thermal correction.
- 17 (a) G. A. Moniz and J. L. Wood, *J. Am. Chem. Soc.*, 2001, **123**, 5095; (b) Z.-J. Li and H. M. L. Davies, *J. Am. Chem. Soc.*, 2010, **132**, 396; (c) Z.-J. Li, V. Boyarskikh, J. H. Hansen, J. Autschbach, D. G. Musaev and H. M. L. Davies, *J. Am. Chem. Soc.*, 2012, **134**, 15497.
- 18 For discussion of dispersion energy, see: P. R. Schreiner, L. V. Chernish, P. A. Gunchenko, E. Y. Tikhonchuk, H. Hausmann, M. Serafin, S. Schlecht, J. E. P. Dahl, R. M. K. Carlson and A. A. Fokin, *Nature*, 2011, **477**, 308.